


M.N. POLIANSKI  
T.R. RIZZO  
O.V. BOYARKIN 

# Efficient, highly selective laser isotope separation of carbon-13

Laboratoire de chimie physique moléculaire, École Polytechnique Fédérale de Lausanne,  
1015 Lausanne, Switzerland

Received: 2 December 2005 / Revised version: 2 February 2006  
Published online: 30 March 2006 • © Springer-Verlag 2006

**ABSTRACT** We recently demonstrated an original approach to highly selective laser isotope separation of carbon-13 that employs vibrational overtone pre-excitation of  $\text{CF}_3\text{H}$  together with infrared multiphoton dissociation [O.V. Boyarkin, M. Kowalczyk, T.R. Rizzo, *J. Chem. Phys.* **118**, 93 (2003)]. The practical implementation of this approach was complicated by the long absorption path length needed for the overtone excitation laser beam. In the present work, we employ a low overtone level for the pre-excitation that shortens this pathway, facilitating engineering of the process. We propose an optimal configuration of the isotope separation scheme and consider a realistic example of a separation unit for isotopic enrichment of carbon-13 to 94%–98%. The photon energy expenditure of 97 eV per separated atom is much lower than that of the current commercial laser technology, making this process economically feasible.


PACS 82.30.Lp; 89.90.+n

## 1 Introduction

While the use of infrared lasers for molecular-based separation of stable isotopes has led to many interesting findings and promising demonstrations [1–7], few laser isotope separation schemes have reached the stage of commercial application [8]. In the case of schemes based on infrared multiphoton excitation, the limitation is their low isotopic selectivity. Physical methods of isotope separation, such as low temperature distillation of CO in the case of carbon, do not alter the working molecule, and this facilitates the implementation of a multi-cycle separation process [9]. Although the selectivity of each cycle is low, the repetition of many separation cycles makes it possible to achieve the high levels of selectivity demanded by the market. Because molecular laser isotope separation techniques that are based on infrared multiphoton dissociation chemically convert the parent molecule into a new species, repetitive cycles can be complicated and costly. Development of a single-stage, energy-efficient, laser separation technique that could produce the high levels carbon-13 enrichment required by the market (above 95% or above 99%) would fill an important niche.

Over the last several years we have developed a highly selective separation scheme for carbon-13 that combines isotopically selective vibrational overtone pre-excitation (OP) of the CH-stretch vibration in  $^{13}\text{CF}_3\text{H}$  followed by selective IRMPD of the pre-excited molecules (Fig. 1) [10–12]. The  $\text{CF}_2$  fragments combine *via* 3-body collisions to form  $\text{C}_2\text{F}_4$ , which can be separated from the starting material. We have demonstrated selectivities up to 9000 (99% enrichment in carbon-13 starting from  $\text{CF}_3\text{H}$  in natural abundance) that can be enhanced at high sample pressure by V-V collisional relaxation [11]. Since our original discovery of this unexpected effect [11], we have taken several steps that significantly increase the yield of the process, bringing it closer to commercial relevance. In particular, overlapping the pre-excitation laser pulse with a short (50 ns) dissociation pulse from a  $\text{CO}_2$  laser allows working pressures of 100–250 mbar while maintaining a high relative dissociation yield and high isotopic selectivity [12].

Despite the high working pressure of the process, the low absorption cross section of the  $3_1$  vibrational band [14] that we originally employed for overtone pre-excitation makes the  $1/e$  absorption length of the pre-excitation beam fairly long (e.g.,  $> 200$  m at 100 mbar), inhibiting the efficient use of photons. Shortening the absorption length can be achieved by pre-exciting lower CH-stretch bands, which have higher absorption cross-sections. Table 1 summarizes the spectroscopic data for the absorption bands of interest. Pre-excitation through the  $2_1$  and  $2_2$  bands are 6.7 and 4.4 times more efficient than use of the  $3_1$  band, and if the high level of selectivity could be maintained, this would lead to a significantly higher performance of the process. Moreover, generation of high-energy, high repetition rate pulses in the region of  $1.7 \mu\text{m}$  (for the  $2_1$  and  $2_2$  bands) seems to be significantly easier than at  $1.14 \mu\text{m}$  (for the  $3_1$  band) using an OPO + OPA system pumped by a Nd:YAG laser, for example. Thus, use of either the  $2_1$  or  $2_2$  band would be highly desirable for simplifying the engineering of the process and increasing its practical relevance. There are, however, two factors that may complicate the use of these bands. First, the isotopic shift of the  $2_1$  and  $2_2$  bands is smaller than that of the  $3_1$  band, and this reduces isotopic selectivity of the pre-excitation step and thus may substantially reduce the overall selectivity of the process. Second, IRMPD of molecules pre-excited to the first overtone level should be less efficient than dissociation of molecules

 Fax: +41-21-693-5170, E-mail: Oleg.Boiarkin@epfl.ch

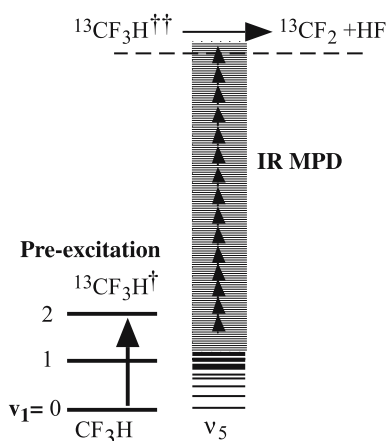


**FIGURE 1** Schematic energy level diagram of the overtone pre-excitation infrared multiphoton dissociation method for highly selective carbon-13 isotope separation using  $\text{CF}_3\text{H}$  as the parent molecule

from the  $3_1$  level, because the former have less vibrational energy. In this paper we present the results of our experiments applying the OP-IRMPD approach for separation of carbon-13 in  $\text{CF}_3\text{H}$ , employing the  $2_1$  and  $2_2$  bands for pre-excitation. We compare these results with those obtained for the  $3_1$  band and evaluate the overall performance of the isotope separation scheme. We also verify that the process can benefit from reducing the intensity of the dissociation laser pulse at fixed fluence, as we have previously suggested [12]. Finally, we estimate the quantum efficiency of the process and consider a potential example of its practical implementation.

## 2 Experimental approach

The experimental set-up, shown in Fig. 2, is identical to that used in the earlier experiments where we employed the  $3_1$  band for pre-excitation [12], except for the method of generating tunable infrared laser radiation. The current system uses difference frequency mixing (DFM) in a nonlinear crystal to generate near IR light and optical parametric amplification (OPA) to achieve high pulse energy. A fraction of the fundamental beam from a single-mode, Nd:YAG laser (Spectra-Physics GCR-250) is frequency-doubled to pump a dye laser (Lambda Physik Scanmate 2E). The 30–40 mJ output of the dye laser is mixed with 150 mJ of the Nd:YAG laser fundamental in a  $\text{LiNbO}_3$  crystal to generate 2–4 mJ of tunable IR radiation. The output of the DFM stage is further amplified in a two-stage OPA pumped by 200–300 mJ

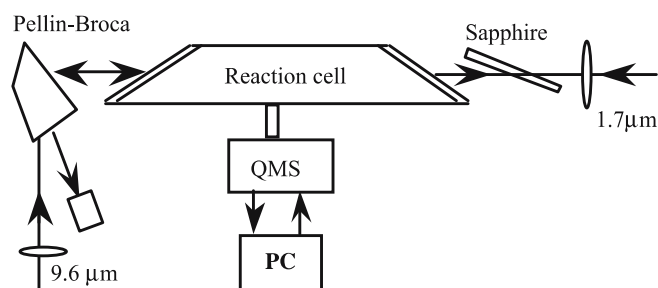


**FIGURE 2** Optical layout of the experiments

Band in $^{13}\text{CF}_3\text{H}$	Transition wavenumber <sup>a</sup> $\text{cm}^{-1}$	Isotopic shift <sup>b</sup> $\nu(^{12}\text{C}) - \nu(^{13}\text{C})$ , $\text{cm}^{-1}$	Absorption cross-section at $T = 300 \text{ K}^c$ , $\text{cm}^2$
$3_1$	8753	39.7	$1.8 \times 10^{-21}$
$2_1$	5936.6	22.8	$12 \times 10^{-21}$
$2_2$	5680.9	29.5	$7.9 \times 10^{-21}$

<sup>a</sup> From [15]; <sup>b</sup> Calculated from [14] and [15]; <sup>c</sup> Calculated considering integral absorption intensities from [14] and our measurements of absorption spectra

**TABLE 1** Spectroscopic data for selected CH-stretch overtone bands of  $^{13}\text{CF}_3\text{H}$

of the infrared fundamental of the same Nd:YAG laser. This results in 120 mJ, 6 ns pulses of tunable around  $1.7 \mu\text{m}$  radiation with  $0.1 \text{ cm}^{-1}$  bandwidth. The pre-excitation laser beam is slightly focused by a telescope before entering the reaction cell through a  $\text{BaF}_2$  window at the Brewster angle. The dissociating  $\text{CO}_2$  laser beam is focused by an  $F = 100 \text{ cm}$  lens and enters the reaction cell from the opposite side. The 50 ns long pulses of this laser overlap the 6 ns pre-excitation pulses. The isotopic composition of the  $\text{C}_2\text{F}_4$  dissociation product is measured by a computer controlled quadrupole mass spectrometer (Balzers, QMS-422) as previously described [12].

## 3 Results

### 3.1 Pre-excitation to the first CH-stretch overtone

The  $Q$ -branches of the  $2_2$  and  $2_1$  CH-stretch overtone transitions in room temperature  $^{13}\text{CF}_3\text{H}$  appear as prominent peaks – an order of magnitude more intense than their

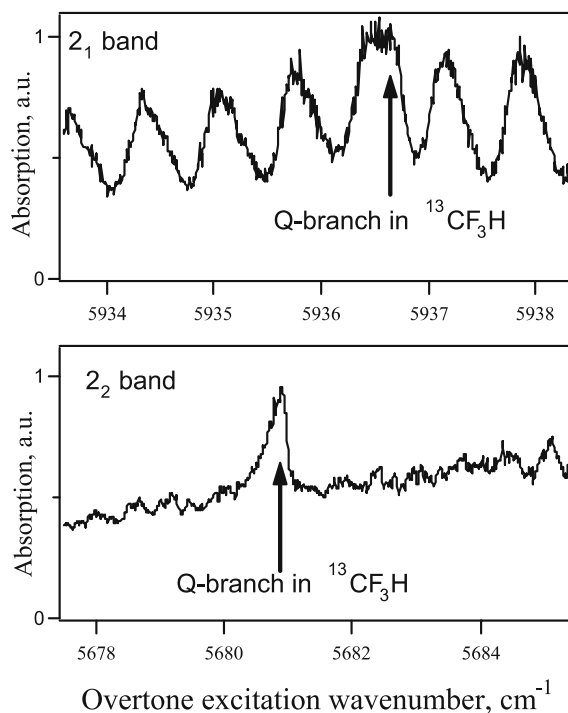


**FIGURE 3** Portions of photoacoustic spectra of the  $2_1$  and  $2_2$  bands in naturally abundant  $\text{CF}_3\text{H}$ . Arrows indicate the maxima of the  $Q$ -branches of these bands in  $^{13}\text{CF}_3\text{H}$  [15]

*P* and *R*-branches [15]. Figure 3 shows the photoacoustic absorption spectra of naturally abundant  $\text{CF}_3\text{H}$  in the regions of the  $2_2$  and the  $2_1$  band *Q*-branches of the carbon-13 species. Because of its larger isotopic shift, the  $2_2$  *Q*-branch of the carbon-13 species is overlapped with high *J* transitions of the *P*-branch in  $^{12}\text{CF}_3\text{H}$ . Due to the splitting of high *J*-states of the  $2_2$  level by weak perturbations [14], these transitions appear unresolved at our moderate spectral resolution of  $0.08\text{ cm}^{-1}$ , forming a nearly continuous background. Given the degree of spectral overlap, the maximum isotopic selectivity that one could expect in the pre-excitation step using the  $2_2$  band is around 90, which is substantially lower than the selectivity of 400 previously measured using the  $3_1$  band [11]. Because of its smaller isotopic shift, the *Q*-branch of the  $2_1$  band in  $^{13}\text{CF}_3\text{H}$  falls into a region of more intense, but resolved, transitions of the carbon-12 species. Here the  $2_1$  *Q*-branch in  $^{13}\text{CF}_3\text{H}$  is adjacent to a single transition. The isotopic selectivity using the  $2_1$  level, estimated by fitting the spectrum in Fig. 3, could be up to 100 if a narrow-bandwidth laser is used for pre-excitation. Because of the particular overlap pattern of these transitions, excitation at the maximum of the  $2_1$  *Q*-branch of  $^{13}\text{CF}_3\text{H}$  will not necessarily yield the highest isotopic selectivity – some optimization of the pre-excitation frequency is required.

Figure 4a and b shows the isotopic selectivity and relative IRMPD yield (i.e., fraction of the pre-excited molecules that have been dissociated) as a function of  $\text{CF}_3\text{H}$  pressure for the OP-IRMPD process with pre-excitation to the  $3_1$  and  $2_2$  bands. In the latter case, the dissociation fluence has been increased to  $4.5\text{ J/cm}^2$  in order to achieve a relative IRMPD yield approximately equal to that obtained with  $3\text{ J/cm}^2$  when the  $3_1$  band is pre-excited. This allows a convenient comparison of the two experiments using a single parameter, isotopic selectivity, which is less ambiguous than the simultaneous comparison of two parameters (selectivity and yield). When extrapolated to zero pressure, the isotopic selectivity with pre-excitation through the  $2_2$  band is about three-fold lower than with pre-excitation through the  $3_1$  band. However, already at sample pressures above 50 mbar, the selectivity in both experiments becomes almost equal, and further increase in pressure does not influence the ratio between them. This suggests that the enhancement of selectivity by collisions is higher in the case of pre-excitation to the lower energy level ( $2_2$ ) compared to that achieved using the  $3_1$  level. Thus, using pre-excitation via the  $2_2$  band and increasing the fluence of the dissociation laser by a factor of 1.5, one can achieve approximately the same overall isotopic selectivity and fraction dissociated in the IRMPD step as with the  $3_1$  band for sample pressures above 50 mbar. However, because the absorption cross-section of the  $2_2$  band is 4.4 times higher than of the  $3_1$  band, the absolute yield of the processes per irradiated unit volume increases by this same factor (Fig. 4c). Therefore, for the same (short) absorption pathway, the overall productivity of the process increases a factor of 4.4 using  $2_2$  versus  $3_1$  as a pre-excitation level.

The productivity is even higher with pre-excitation through the  $2_1$  band. At 100 mbar we observe an increase in the per volume dissociation yield by a factor of 1.5 compared to the  $2_2$  band, which reflects the ratio of the  $2_1$  to  $2_2$  absorption cross sections. While there is a decrease in the pre-excitation

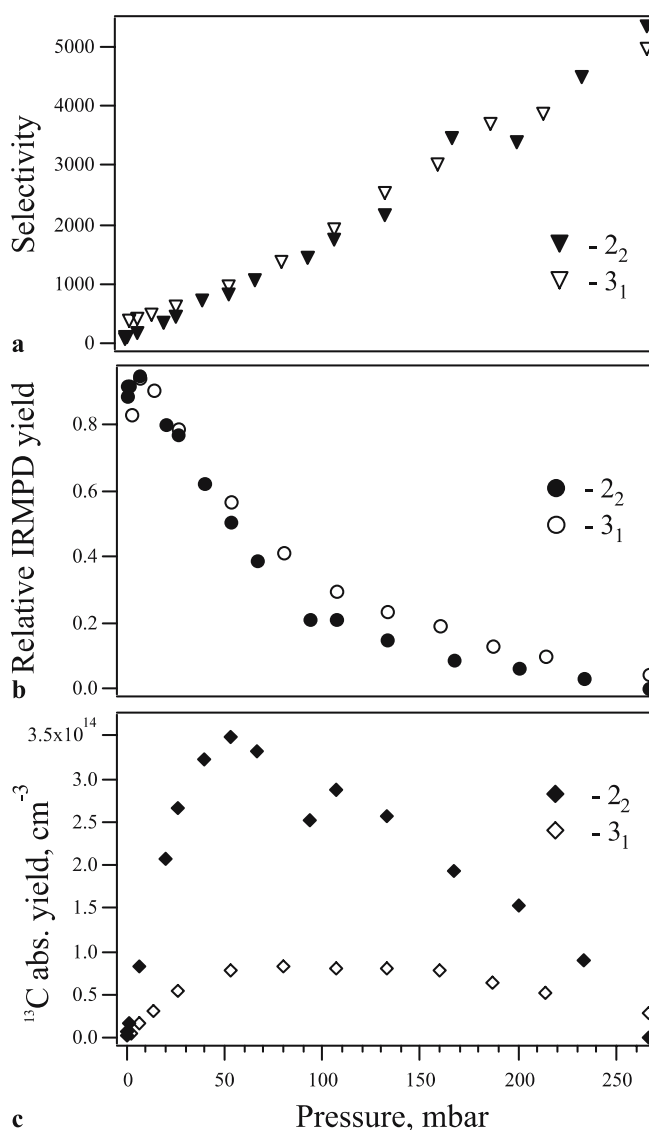


**FIGURE 4** Isotopic selectivity (a), relative IRMPD yield (b) and the absolute yield (c) as a function of  $\text{CF}_3\text{H}$  pressure in the case of pre-excitation to the  $2_2$  level (filled markers) and the  $3_1$  level (open markers). The absolute yield is given in units of  $^{13}\text{C}$  atoms per  $\text{cm}^3$  and per  $\text{J/cm}^2$  pre-excitation fluence. The dissociation fluence is  $4.5\text{ J/cm}^2$  and  $3\text{ J/cm}^2$  for the  $2_2$  and  $3_1$  bands respectively. The pre-excitation and dissociation pulses are overlapped in time

selectivity of less than 10% in changing the level from  $2_2$  to  $2_1$ , it can be regained by increasing the sample pressure, although with 10% decrease of dissociation yield. Thus, for a fixed isotopic selectivity and a fixed laser beam pathway, the process yield with pre-excitation through the  $2_1$  band is 1.35 times higher than pre-excitation through the  $2_2$  band and about six times higher than with the  $3_1$  band employed previously. In what follows we thus concentrate on experiments employing pre-excitation through the  $2_1$  band.

### 3.2 Dissociation by a temporally modified $\text{CO}_2$ laser pulse

The output beam of our free-running  $\text{CO}_2$  laser appears as a train of 1–2 ns pulses separated by the cavity

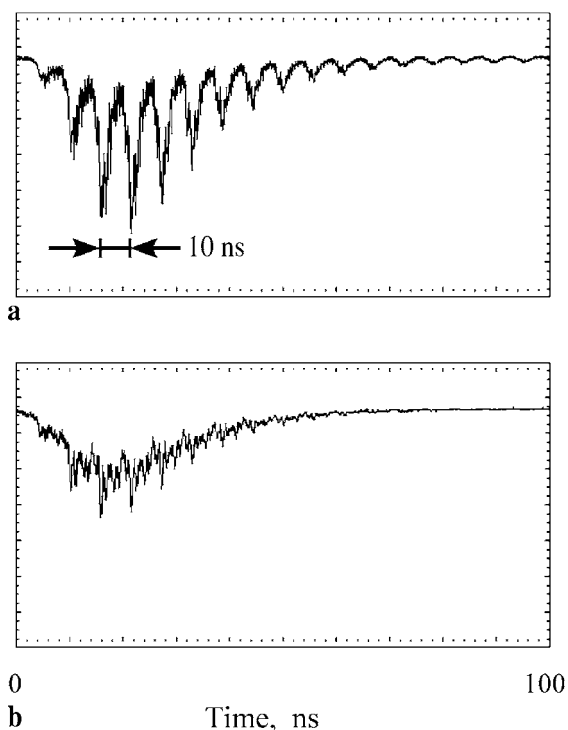


**FIGURE 5** Oscilloscope traces of the regular (a) and the “doubled” (b) dissociation  $\text{CO}_2$  laser pulses obtained with 2 ns resolution

round trip time of 10 ns (Fig. 5a) as a result of self mode-locking [16]. This spiky structure of the  $\text{CO}_2$  laser pulse imposes a certain time structure on the multiphoton absorption process, which competes with collisions. Considering the competition between up-pumping and collisional V-V relaxation [12], there should be a predominance of up-pumping during a laser intensity spike and of relaxation in the short time between the spikes. Thus, the entire process of multiphoton excitation consists of a number of short, repetitive subprocesses that limit the possibility of increasing the sample pressure with simultaneous increase of dissociation laser fluence. Indeed, if the collisional relaxation rate is too high, during the time-delay between two laser spikes the pre-excited molecules may relax below the energy where efficient IR multiphoton pumping can occur. Increasing the dissociation laser fluence to compensate this will increase the probability for dissociation of both the relaxed and the ground state carbon-12 species. It is clear that for the efficient use of the competition between up-pumping and collisional V-V relaxation during the  $\text{CO}_2$  laser pulse, the distance between the adjacent spikes should not considerably exceed the average time between two subsequent collisions. We previously measured a value of  $5\text{--}7\ \mu\text{s}^{-1}\text{mbar}^{-1}$  for the vibrational relaxation rate constant of the first CH-stretch overtone level in  $\text{CF}_3\text{H}$  [11], which is close to the recently calculated value of  $5\ \mu\text{s}^{-1}\text{mbar}^{-1}$  [13]. Given this rate constant, one can see that already at  $\text{CF}_3\text{H}$  pressures above 20 mbar, the spiky structure of the dissociation pulse has a considerable destructive influence on the performance of the process. A smooth temporal pulse shape would thus be highly desirable. This can be achieved by forcing the dissociation laser to oscillate on a single longitudinal mode by one of several means: injection seed-

ing; using a combination of a high-pressure discharge region with a low pressure gain section; or by using an intra-cavity cell with a selective absorber, each of which would require rebuilding our  $\text{CO}_2$  laser. To demonstrate the influence of laser pulse shape, we have chosen a simple approach that modifies the shape of our laser pulses outside of the laser cavity. Although this approach cannot be used in a large-scale apparatus, its simplicity and pulse-to-pulse reproducibility makes it convenient for laboratory experiments with a small working volume. The  $\text{CO}_2$  laser beam is split to two beams of nearly equal intensity by a ZnSe beam splitter. One of the two beams is optically delayed by 5 ns with respect to the other split beam. Both beams are then focused by the same  $F = 100\ \text{cm}$  ZnSe lens and overlap in the 2 cm long reaction cell. This has the effect of interposing spikes in the pulse of one beam precisely between those of the other, shortening the delay between spikes that the molecules experience from 10 ns to 5 ns. Figure 5 shows the temporal profile of a pulse emanating from the  $\text{CO}_2$  laser and the profile of the “doubled” pulse, measured using a Ge photon drag with 1 ns time resolution. Although the spiky structure in such “doubled” pulses has not been completely smoothed, we still can draw conclusions about the potential advantages of using a truly “smooth” dissociation laser pulse in our isotope separation process.

The yield and selectivity of the OP-IRMPD process using  $2_1$  pre-excitation is shown in Fig. 6 as a function of the sample pressure for the regular and “doubled” dissociation laser pulses at a dissociation laser fluence of  $3\ \text{J}/\text{cm}^2$ . As the figure illustrates, the “doubled” pulses cause a slower increase of isotopic selectivity and slower decrease of dis-

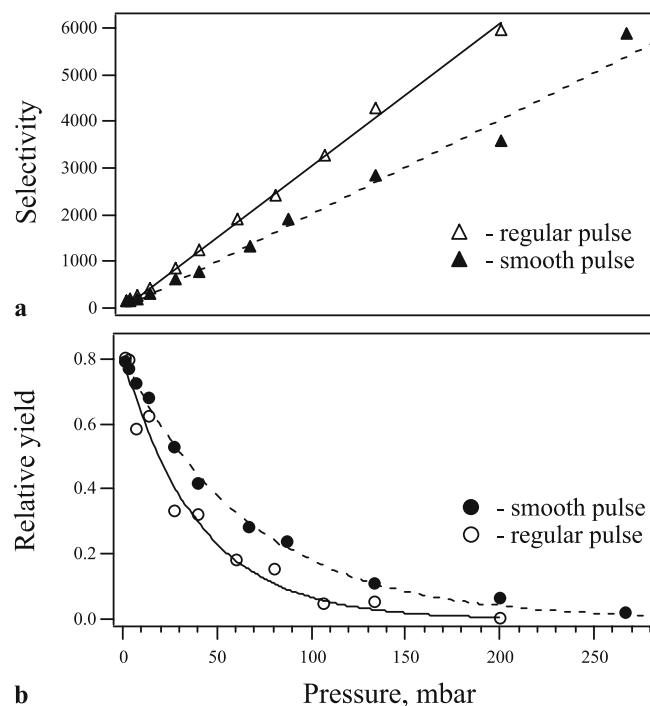


**FIGURE 6** Isotopic selectivity (a) and relative IRMPD yield (b) as a function of  $\text{CF}_3\text{H}$  pressure in the case of pre-excitation to the  $2_1$  level by the regular (opened markers) and smoothed (filled markers) dissociation pulses. The pre-excitation fluence is  $1\ \text{J}/\text{cm}^2$ , and the dissociation fluence is  $3\ \text{J}/\text{cm}^2$ . The pre-excitation and dissociation pulses are overlapped in time

sociation probability upon increase of  $\text{CF}_3\text{H}$  pressure compared to the regular  $\text{CO}_2$  laser pulses. The effect is similar to what one would observe by increasing the fluence of a regular pulse [12]. A certain value of isotopic selectivity achieved either with the smoothed, “doubled” pulse or with the intense, regular pulse corresponds to the same relative IRMPD yield. To achieve, for example, isotopic selectivity of 2000 (95.4% of carbon-13 in the final product), one can use either the regular  $\text{CO}_2$  laser pulses and a pressure of 65 mbar or the smoothed pulses and 100 mbar. In both cases approximately 18% of pre-excited molecules are dissociated. However, working at higher pressure is advantageous from point of view of absolute productivity of the process. For the fixed selectivity of 2000, the absolute productivity per irradiated volume unit (per volume productivity) with our smoothed pulse is 1.5 times higher than for the regular (self-mode locked)  $\text{CO}_2$  laser pulse. We believe that the use of a truly smooth pulse shape would increase the productivity even further.

### 3.3 Absorption of $\text{CO}_2$ laser radiation by pre-excited molecules

The dissipation of vibrational energy of pre-excited carbon-13 species by collisions implies that the average number of absorbed  $\text{CO}_2$  laser photons per molecule is higher than energetically necessary for dissociation (19 photons from the  $2_1$  level, for example). Moreover, some of the pre-excited molecules may not absorb enough  $\text{CO}_2$  laser photons to dissociate. This will further increase the average number of photons absorbed per dissociated molecule. The number of photons actually absorbed is a key to evaluate the minimum energy expenditure per separated atom and the characteristic absorption length of the dissociation laser beam, the latter of which should be matched to that of the pre-excitation laser beam. This number thus highly influences the practical design of the process and, ultimately, the productivity of a separation unit.

In order to estimate the average number of  $\text{CO}_2$  laser photons absorbed per pre-excited molecule under the typical conditions of the separation process, we measured the  $\text{CO}_2$  laser energy absorbed by  $\text{CF}_3\text{H}$  molecules pre-excited to the  $2_1$  level. In this experiment, a near collimated  $\text{CO}_2$  laser beam of 2–3  $\text{J}/\text{cm}^2$  fluence is counter-propagated with a pre-excitation beam of larger diameter in the 50 cm long cell, which is filled with 100 mbar of  $\text{CF}_3\text{H}$ . A small fraction of the dissociation beam is split after the cell and sent to a pyroelectric detector. The  $\text{CO}_2$  laser is tuned to the  $9P(14)$  line at  $1052.2\text{ cm}^{-1}$ , where the absorption cross-section of ground state  $\text{CF}_3\text{H}$  has an absorption minimum [17]. The fluence of the pre-excitation laser is 1  $\text{J}/\text{cm}^2$ , which promotes  $\sim 10\%$  of the irradiated  $^{13}\text{CF}_3\text{H}$  to the  $2_1$  level. Absorption of the dissociation laser beam by the pre-excited molecules is measured as the difference between the detector signals with and without the pre-excitation pulse. The detected induced absorption is  $\sim 2\%$ , which corresponds to a characteristic absorption length of 25 m. Taking into account the concentration of pre-excited  $^{13}\text{CF}_3\text{H}$  in the irradiated volume, we estimate the average number of  $\text{CO}_2$  laser photons absorbed by each pre-excited molecule to be  $36 \pm 6$ .

## 4 Discussion

The experimental results reported here and in the previous paper [12] enable us to optimize the configuration of our OP-IRMPD scheme for highly selective separation of carbon-13 using  $\text{CF}_3\text{H}$ . We evaluate below the maximum possible productivity and the minimum necessary energy expenditure per separated atom for an ideal separation unit based on this configuration.

The optimal configuration of the separation scheme depends largely on the required level of isotopic enrichment. Although we have demonstrated carbon-13 enrichment levels as high as 99% [11], it seems that the most appropriate use of this method would be for enrichment levels of 94%–98%. To maximize the per volume productivity at these enrichment levels, one should use the  $2_1$  level for pre-excitation. A short (few tens of ns), single-mode dissociation laser pulse should overlap the pre-excitation pulse in time. As we observed earlier [12], such temporal arrangement significantly increases the dissociation yield at high sample pressure. A dissociation laser fluence of approximately 3  $\text{J}/\text{cm}^2$  gives a reasonably high yield, but is still lower than the damage threshold of many IR materials, enabling the use of unfocussed, collimated beams. This is essential, since it allows irradiation of large volumes over a long path length. For optimal use of laser photons, the absorption lengths for the two laser beams should be nearly equal. The required selectivity essentially determines the working pressure of the process and, therefore, the absorption length of the pre-excitation beam. However, the absorption length of the dissociation beam is also determined by the fraction of pre-excited molecules – that is, by fluence of the pre-excitation laser. This puts some constraints on the latter.

Let us consider a particular example. Suppose the targeted level of enrichment is 95.4%, which corresponds to selectivity of 2000. Figure 6 suggests that with a smooth dissociation pulse of 3  $\text{J}/\text{cm}^2$ ; this selectivity requires about 100 mbar of  $\text{CF}_3\text{H}$ . The characteristic absorption length for pre-excitation beam  $L_p$  is given as

$$L_p = \frac{1}{n_{13}\sigma_{13}^p(1 + 99/S_p)}, \quad (1)$$

where  $n_{13}$  is concentration of  $^{13}\text{CF}_3\text{H}$ ,  $\sigma_{13}^p$  is absorption cross-section for the  $Q$ -branch of the  $2_1$  band and  $S_p = 85$  is the measured selectivity of pre-excitation. At 100 mbar and with  $\sigma_{13}^p = 1.2 \times 10^{-20}$  (Table 1), (1) yields a characteristic absorption length for the pre-excitation beam of 14.3 m. Attenuation of the dissociation beam to the  $1/e$  level by the pre-excited molecules occurs over length  $L_d^\star$ , given as

$$L_d^\star = \frac{(e - 1) \Phi_d \lambda_d}{\langle N_d \rangle n_{13} \sigma_{13}^p \Phi_p, \lambda_p} \quad (2)$$

Here,  $\Phi_d = 3\text{ J}/\text{cm}^2$ ,  $\lambda_d = 9.5\text{ }\mu\text{m}$ ,  $\Phi_p, \lambda_p = 1.7\text{ }\mu\text{m}$  are the fluence and the wavelength of the dissociation and the pre-excitation beams respectively, and  $\langle N_d \rangle = 36$  is the average number of photons absorbed per each pre-excited molecule. We also have to take into account the absorption of this beam by the ground state molecules,

$$L_d^0 = \frac{1}{n\sigma^d}; 80\text{m} \quad (3)$$

where  $L_d^0$  is the characteristic absorption length,  $n$  is the total concentration of  $\text{CF}_3\text{H}$  and  $\sigma^d = 0.47 \times 10^{-22}$  is the absorption cross-section of the ground state  $\text{CF}_3\text{H}$  at the dissociation wavenumber ( $1052.2 \text{ cm}^{-1}$ ) [17]. Within the typical pressure and fluence ranges used in our experiments, this absorption remains a linear function of these parameters [17].

The required balance between absorption lengths for the two laser beams implies

$$\frac{1}{L_p} \cong \frac{1}{L_d^0} + \frac{1}{L_d^\star}. \quad (4)$$

Solving (2)–(4) relative to the pre-excitation fluence yields its optimal value of  $1.4 \text{ J/cm}^2$ . We assume that the pre-excitation beam with pulse energy of  $1.4 \text{ J}$  and  $1 \text{ cm}^2$  cross-section is overlapped with a similar dissociation beam of  $3 \text{ J}$  pulse energy inside a  $15 \text{ m}$  long reactor (or a shorter one with multiple passes). If the beams are slightly focused such that their respective fluence remains constant along their pathways, then the maximum irradiated volume of the reactor will be around  $400 \text{ cm}^3$ . These optimal fluences result in pre-excitation of nearly 14% of irradiated  $\text{CF}_3\text{H}$  molecules, of which nearly 18% will be dissociated (Fig. 6b). At a pressure of  $100 \text{ mbar}$ , the productivity of such a separation unit per pair of laser pulses can reach  $2.8 \times 10^{17}$  atoms of carbon-13 in the chemical form of  $\text{C}_2\text{F}_4$  at 95.4% isotopic purity. The main parameters of the considered separation unit are summarized in Table 2.

An important characteristic of any isotope separation process is the energy expenditure per separated atom. This value gives a lower limit for energy consumption and, thus, the minimum running cost of the process. The photon energy expenditure by the pre-excitation laser per separated carbon-13 atom, calculated as a ratio of the pulse energy of this laser to the per pulse productivity of the separation unit (Table 2) is  $31 \text{ eV}$ . Similar calculation yields  $66 \text{ eV}$  for the energy expenditure by the dissociation laser. The minimum energy expenditure using our process to achieve isotopic selectivity of 2000 is, thus,  $97 \text{ eV}$  per carbon-13 atom. This can be compared to the energy expenditure in the ‘classical’ laser isotope separation of carbon-13 by IRMPD of  $\text{CF}_2\text{HCl}$ . Enrichment to a similar (96%) level of carbon-13 requires  $760 \text{ eV}$  of laser energy per carbon atom [3]. Clearly, for high levels of isotopic enrichment our laser isotope separation process is by far superior to the ‘classical’ IRMPD of  $\text{CF}_2\text{HCl}$  from

the point of view of the minimum possible photon energy expenditure.

Enrichment of carbon-13 by low-temperature distillation of  $\text{CO}$ , currently the main commercial production technology consumes up to  $1500 \text{ eV/C}$  – atom of energy in the form of liquid nitrogen [18]. Whether the technology based on our approach will consume less energy depends primarily on the efficiency of the lasers employed. The electrical efficiency of pulsed  $\text{CO}_2$  lasers is typically 10%, bringing the energy consumption by the dissociation laser in our process to  $660 \text{ eV/atom}$ . Thus, to be competitive with the distillation process, the energy consumption by the pre-excitation laser has to be below  $900 \text{ eV/atom}$ , which means that the efficiency of this laser should be above 3.5%. The development of an efficient, high repetition rate, high-energy near-IR laser system seems challenging, but currently realistic. This could be an all solid-state system based on a diode-pumped Nd:YAG laser and an OPO/OPA wavelength converter. The efficiency of such laser system can approach 5%–10%. At 10%, this would imply that our laser isotope separation approach for carbon-13 would be approximately 1.5 times more efficient than low temperature distillation of  $\text{CO}$ .

## 5 Conclusions

We have further developed our collisionally assisted overtone pre-excitation-IRMPD approach to highly selective laser isotope separation of carbon-13 using  $\text{CF}_3\text{H}$  as a starting material. Employing the  $2_1$  vibrational level for pre-excitation, which has 6.7 times higher absorption cross-section than the previously used  $3_1$  level, allows for a significant increase of per volume absolute dissociation yield. Although the isotopic selectivity using pre-excitation of  $\text{CF}_3\text{H}$  to the former level is several times lower than that for the latter, collisional V-V relaxation quickly compensates this difference upon increase of pressure to above  $50 \text{ mbar}$ . Smoothing the spiky structure of pulses delivered by our  $\text{CO}_2$  laser allows for the further increase of the per volume absolute dissociation yield.

We suggest an optimal configuration of the process that includes pre-excitation to the  $2_1$  level by a short (10–30 ns) pre-excitation pulse and a slightly longer single-mode dissociation pulse, overlapped in time. The investigated approach is most appropriate for carbon-13 enrichment to the level of 94%–98%. An example of an ideal separation unit illustrates the attainable performance of the process. The estimated productivity at an enrichment level of 95.4% is  $2.8 \times 10^{17}$  carbon-13 atoms per pair of laser pulses using  $1.4 \text{ J/pulse}$  for the pre-excitation laser and  $3 \text{ J/pulse}$  for dissociation laser.

The evaluated energy expenditure,  $97 \text{ eV}$  per separated carbon-13 atom, is several times less than for the classical laser separation technique using IRMPD of  $\text{CF}_2\text{HCl}$ . The main challenge for practical implementation of our process is the development of the required pre-excitation laser system with at least 3.5% of photon/electrical power efficiency. With such a laser and when properly engineered, the process should be competitive with the current carbon-13 separation technologies.

Parameter	Value
Pre-excitation wavenumber, $\text{cm}^{-1}$	5936.6
Pre-excitation energy, J	1.4
Dissociation wavenumber, $\text{cm}^{-1}$ ( $\text{CO}_2$ laser line)	1052.2 (9P)
Dissociation energy, J	3
$\text{CF}_3\text{H}$ pressure, mbar	100
Length of the dissociation volume, m	15
Dissociation volume, $\text{cm}^3$	400
Productivity, $^{13}\text{C}$ atoms per pair of laser pulses	$2.8 \times 10^{17}$
Energy expenditure per separated $^{13}\text{C}$ atom, eV	97

TABLE 2 The principal parameters of the separation cell

**ACKNOWLEDGEMENTS** The authors thank Dr. Richard Bossart for his help in some of the experiments. The authors gratefully acknowledge the financial support of this work by the Fonds National Suisse through grant 200020-101475, Silex Systems Ltd. and the EPFL.

## REFERENCES

- 1 M. Droun, M. Gauthier, R. Pilon, P.A. Hackett, C. Willis, *Chem. Phys. Lett.* **60**, 16 (1978)
- 2 V.N. Bagratashvili, V.S. Doljikov, V.S. Letokhov, E.A. Ryabov, *Appl. Phys.* **20**, 231 (1979)
- 3 M. Gauthier, C.G. Cureton, P.A. Hackett, C. Willis, *Appl. Phys. B* **28**, 43 (1982)
- 4 A.V. Evseev, V.S. Letokhov, A.A. Puretsky, *Appl. Phys. B* **36**, 93 (1985)
- 5 W. Fuss, J. Göthel, M. Ivanenko, K.L. Kompa, W.E. Schmid, *Z. Phys. D* **24**, 47 (1992)
- 6 V.N. Lohman, G.N. Makarov, E.A. Ryabov, M.V. Sotnikov, *Kvantovaya Elektronika* **23**, 81 (1996)
- 7 V.M. Apatin, V.P. Laptev, E.A. Ryabov, *High Energ. Chem.* **37**, 101 (2003)
- 8 V.Y. Baranov, A.P. Dyadkin, D.D. Maluta, V.A. Kuzmenko, S.V. Pigulski, I.V. Yarovoi, V.B. Zarin, A.S. Podoryashy, *Laser Separation Complex "Carbon"* (CNIIatominform, Zvenigorod, Russia, 1999)
- 9 B.B. McInteer, *Sep. Sci. Technol.* **15**, 491 (1980)
- 10 T. Rizzo, O. Boiarkine, USA Patent No. US 6653587, B1 (1999)
- 11 O.V. Boyarkin, M. Kowalczyk, T.R. Rizzo, *J. Chem. Phys.* **118**, 93 (2003)
- 12 M. Polianski, O.V. Boyarkin, T.R. Rizzo, *J. Chem. Phys.* **121**, 11771 (2004)
- 13 R. Bossart, PhD thesis N<sup>o</sup> 3298, Lausanne, EPFL (2005)
- 14 H.-R. Dübal, M. Quack, *J. Chem. Phys.* **81**, 3779 (1984)
- 15 H. Hollenstein, M. Lewerenz, M. Quack, *Chem. Phys. Lett.* **165**, 175 (1990)
- 16 W.J. Witteman, *The CO<sub>2</sub> Laser* (Springer-Verlag, Berlin Heidelberg, 1987)
- 17 J.A. O'Neill, L. Pateopol, B. Pogue, *J. Phys. B At. Mol. Opt.* **25**, 3335 (1992)
- 18 D. Stachewski, *Chem. Tech.* **4**, 269 (1975)